Chapter 30

The PING model of gamma rhythms

When populations of excitatory and inhibitory neurons are synaptically connected, oscillations often emerge. The reason is apparent: Activity of the excitatory neurons (which we will call *E-cells* from here on, as we did in Chapter 22) generates activity of the inhibitory neurons (*I-cells*). The activity of the I-cells causes the activity of the E-cells to cease transiently, and when it resumes, the E-cell population is closer to synchrony, as discussed in Chapter 29.[24] The oscillations in Chapter 22 are of a similar nature, although there individual cells were not modeled. Figure 30.1 (nearly identical with Fig. 22.1) represents the interaction of E- and I-cells symbolically.
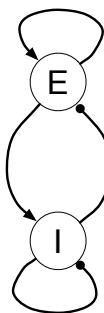
Figure 30.1. *Symbolic depiction of a network of E- and I-cells. The large circles labeled "E" and "I" represent* populations *of cells. Lines ending in arrows indicate excitation, and lines ending in solid circles indicate inhibition.*

In particular, brain oscillations with frequencies of about 30–80 Hz are thought

---

[24]This requires that input from the I-cells in fact delays and synchronizes E-cell firing. For example, an h-current in the E-cells can undermine the mechanism, since hyperpolarization turns on the h-current, which is depolarizing. However, in this chapter, we will take the E-cells to be RTM neurons, for which no such complications arise.

to arise in this way in many instances. Oscillations in the 30–80 Hz frequency range are called *gamma oscillations* or *gamma rhythms*. They are seen in EEG traces and in local field potentials, and are correlated with perception, attention, and memory; for a review, see for instance [18]. A connection between meditation and gamma rhythms has been documented several times; see for instance [107]. Pathologies in gamma rhythms are associated with schizophrenia [62, 127, 144]. Notwithstanding these observed correlations, it is not universally agreed upon that gamma rhythms (or rhythms in any frequency band) play an important role in coding or information processing in the brain; see for instance [128]. Here we will focus on how gamma rhythms may arise, and make no claims about their function. Results potentially pertinent for their function will be presented in Chapters 35–38.

The E- and I-cells believed to generate gamma rhythms are pyramidal neurons and fast-firing PV+ interneurons. Rhythms of this kind are therefore referred to as *pyramidal-interneuronal network gamma (PING)* rhythms. The acronym PING goes back at least to Traub *et al.* [161]; the observation that gamma rhythms can be generated in this way goes back further; see for instance [43, 84, 93, 157].

A natural question arises here: What is special about the gamma frequency? Why can't the interaction of E- and I-cells generate oscillations at any frequency? In fact it can. For instance, [173] describes oscillations in a model network at frequencies around 10 Hz arising from the interaction of excitatory and inhibitory cell populations. These oscillations model *sleep spindles*, oscillations that appear in the EEG during *stage 2 sleep*. The frequency of an oscillation in an *E-I-network* (a network of excitatory and inhibitory neurons) depends in general on the strength and duration of the inhibitory synaptic currents that impose the breaks between population spike volleys, as well as on the external drive. In the network of [173], for instance, there are slow, $GABA_B$-receptor-mediated inhibitory synapses. The decay time constant of $GABA_A$ receptor-mediated inhibitory synapses has been reported in some places to be on the order of 10 ms [69, 136], and the gamma period (approximately 12 to 33 ms) is a small multiple of this value; this may suggest that $GABA_A$ receptor-mediate inhibition will tend to generate oscillations in the gamma frequency range. However, the strength of the inhibitory synapses and especially the external drive contribute significantly to setting the frequency; see Table 29.2, and also Table 30.1.

Experimental evidence supports the idea that the PING mechanism often underlies gamma rhythms. One of many examples is reproduced in Fig. 30.2, which shows recordings from the *CA1* area of rat hippocampus. (Areas *CA1*, *CA2*, and *CA3* are subdivisions of the hippocampus. "CA" stands for "cornu Ammonis", the horn of the ancient Egyptian god Amun. *Cornu ammonis* is an 18th-century term for a part of the hippocampal formation.) The figure demonstrates that during gamma rhythms triggered by *tetanic stimulation* (stimulation by a high-frequency train of electrical pulses) in CA1, both pyramidal cells and inhibitory interneurons fire at approximately gamma frequency.
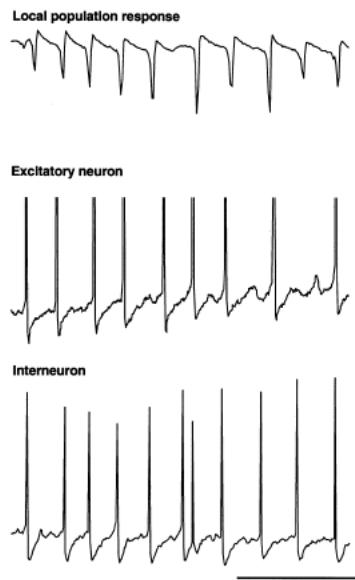
Figure 30.2. *Figure 5 of [181]. These are recordings from the CA1 region of rat hippocampus. Gamma oscillations are triggered by* tetanic stimulation, *i.e., by a high-frequency train of stimulating electrical pulses. Tetanic stimulation leads to the depolarization of both pyramidal neurons and inhibitory interneurons, as a result of* metabotropic glutamate receptor *activation [178]. The figure shows a local field potential (top trace), and membrane potentials of a pyramidal cell and an inhibitory interneuron (middle and bottom traces). The three traces were not recorded concurrently. The horizontal scale bar indicates 100 ms. The vertical scale bars indicate 1 mV (top trace), 4 mV (middle trace), and 20 mV (bottom trace). Reproduced with publisher's permission.*

30.1 Two-cell PING

To build intuition, we begin with a two-cell network, consisting of a single E- and a single I-cell, with E-to-I and I-to-E (but not E-to-E or I-to-I) connectivity. The E-cell is an RTM neuron, and the I-cell a WB neuron. Voltage traces resulting from a simulation of such a two-cell network are shown in Fig. 30.3; the parameter values are specified in the caption of the figure. (Note that we use the notation $\tau_{d,E}$ for the decay time constant of the excitatory synapse, and $\tau_{d,I}$ for that of the inhibitory synapse.) Each time the E-cell fires, the I-cell promptly responds.

We denote the period at which each of the two cells in Fig. 30.3 fires by P, and explore the parameter dependence of P. In analogy with Tables 29.1 and 29.2, we compute the percentage change in P resulting from a 1% reduction in I_E, a 1% increase in $\overline{g}_{IE}$, and a 1% increase in $\tau_{d,I}$. By this measure, the period of the

voltage traces of E-cell (red) and I-cell (blue)
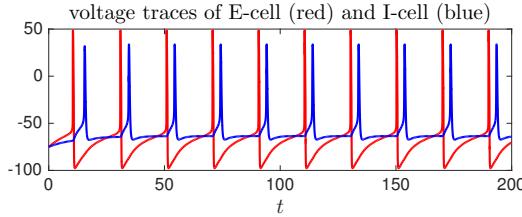
Figure 30.3. *Voltage traces of the two neurons of a network consisting of one RTM and one WB neuron. The external drives are $I_E = 1.4$ and $I_I = 0$. The parameters characterizing the E-to-I and I-to-E synapses are $\overline{g}_{EI} = \overline{g}_{IE} = 0.25$, $\tau_r = \tau_{\text{peak}} = 0.5$ for both synapses, $\tau_d = \tau_{d,E} = 3$ for the E-to-I synapse, and $\tau_d = tau_{d,I} = 9$ for the I-to-E synapse. There are no E-to-E or I-to-I synapses.* [2_CELL_PING]

rhythm depends far more sensitively on external drive than on the strength or decay time constant of inhibition.

	$I_E \to 0.99 I_E$	$\overline{g}_{IE} \to 1.01\overline{g}_{IE}$	$\tau_{d,I} \to 1.01\tau_{d,I}$
increase in P:	0.66%	0.10%	0.14%

Table 30.1. *Parameter dependence of the period P of the rhythm of Fig. 30.3.* [2_CELL_PING_CONDITION_NUMBERS]

30.2 Basic network simulations

In this section, we study numerical results obtained with a network code similar to the one that we used in [91], but using the synaptic model of Section 20.2. (In [91], we used the model of Section 20.1.) The code simulates a network of N_E RTM neurons (E-cells), and N_I WB neurons (I-cells). The numbers N_E and N_I are parameters specified by the user of the code. We usually take N_E to be four times bigger than N_I, since this is often said to be the approximate ratio of glutamatergic to GABAergic neurons in the brain [135]. However, the ratio N_E/N_I is not of great importance for the properties of PING rhythms if the synaptic strengths are scaled as described below.

For each neuron in the network, we define a constant drive I. Different neurons are allowed to have different drives. For any pair of neurons, A and B, in the network, we define parameters associated with a synapse from A to B (compare Section 20.2):

$$\overline{g}_{\text{syn}}, \quad v_{\text{rev}}, \quad \tau_r, \quad \tau_{\text{peak}}, \quad \tau_d.$$

The maximal conductance $\overline{g}_{\text{syn}}$ is allowed to be zero, so not all possible connections are necessarily present. For simplicity, we do not allow the possibility of two different synapses from A to B, for instance a faster and a slower one, here.

In the examples of this section, the parameters are chosen as follows. The i-th E-cell receives input drive

$$I_{E,i} = \overline{I}_E(1 + \sigma_E X_i), \tag{30.1}$$

where $\overline{I}_E$ and $\sigma_E \geq 0$ are fixed numbers, and the X_i are independent standard Gaussian random variables (see Appendix C). Similarly, the j-th I-cell receives input drive

$$I_{I,j} = \overline{I}_I(1 + \sigma_I Y_j), \tag{30.2}$$

where the Y_j are independent standard Gaussians. To set the strengths (maximal conductances) of the synaptic connections from E-cells to I-cells, the *E-to-I connections*, we choose two parameters, $\hat{g}_{EI} \geq 0$ and $p_{EI} \in (0,1]$. The maximal conductance associated with the i-th E-cell and the j-th I-cell is then

$$\overline{g}_{EI,ij} = \frac{\hat{g}_{EI} Z_{EI,ij}}{p_{EI} N_E}, \tag{30.3}$$

where the $Z_{EI,ij}$ are independent random numbers with

$$Z_{EI,ij} = \begin{cases} 1 & \text{with probability } p_{EI}, \\ 0 & \text{otherwise.} \end{cases}$$

The total number of excitatory synaptic inputs to the j-th I-cell is

$$\sum_{i=1}^{N_E} Z_{EI,ij}. \tag{30.4}$$

The expected value of this number is $p_{EI} N_E$ (exercise 2), the denominator in (30.3). Consequently $\hat{g}_{EI}$ is the expected value of the sum of all maximal conductances associated with excitatory synaptic inputs into a given I-cell (exercise 3). Similarly, the strength of the synaptic connection from the j-th I-cell to the i-th E-cell is

$$\overline{g}_{\text{syn},IE,ji} = \frac{\hat{g}_{IE} Z_{IE,ji}}{p_{IE} N_I}, \tag{30.5}$$

with

$$Z_{IE,ji} = \begin{cases} 1 & \text{with probability } p_{IE}, \\ 0 & \text{otherwise.} \end{cases}$$

The strengths of the E-to-E and I-to-I synapses are set similarly.

We use the same values of τ_r, τ_{peak}, τ_d, and v_{rev} for all excitatory synapses. We denote these values by $\tau_{r,E}$, $\tau_{\text{peak},E}$, $\tau_{d,E}$, and $v_{\text{rev},E}$. Similarly, all inhibitory synapses are characterized by parameters $\tau_{r,I}$, $\tau_{\text{peak},I}$, $\tau_{d,I}$, and $v_{\text{rev},I}$.

Figure 30.4 shows the result of a typical network simulation. Starting with E-cell initialized asynchronously, as described in Section 24.1, oscillations at approximately 45 Hz develop rapidly, within about 50 ms. Human reaction times are about 200 to 250 ms, so if gamma rhythms are important for stimulus processing [18], then it must be possible to generate these oscillations in a time much shorter than 200 ms, as indeed seen in Fig. 30.4. In fact, we gave an argument in [16]
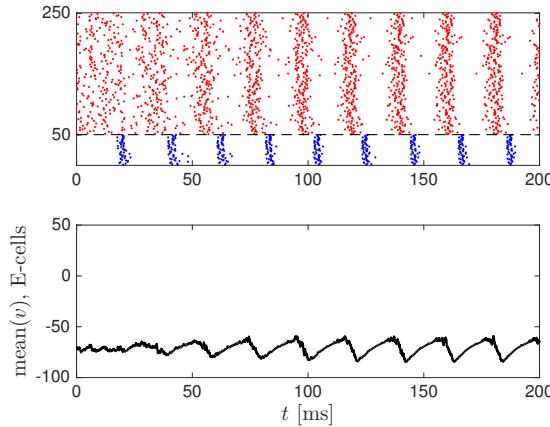
Figure 30.4. *Spike rastergram of a PING network (top), and mean membrane potential of the E-cells (bottom). Spike times of E-cells are indicated in red, and spike times of I-cells in blue. The parameters are $N_E = 200$, $N_I = 50$, $\overline{I}_E = 1.4$, $\sigma_E = 0.05$, $\overline{I}_I = 0$, $\hat{g}_{EE} = 0$, $\hat{g}_{EI} = 0.25$, $\hat{g}_{IE} = 0.25$, $\hat{g}_{II} = 0.25$, $p_{EI} = 0.5$, $p_{IE} = 0.5$, $p_{II} = 0.5$, $\tau_{r,E} = 0.5$, $\tau_{\mathrm{peak},E} = 0.5$, $\tau_{d,E} = 3$, $v_{\mathrm{rev},E} = 0$, $\tau_{r,I} = 0.5$, $\tau_{\mathrm{peak},I} = 0.5$, $\tau_{d,I} = 9$, $v_{\mathrm{rev},I} = -75$.* [`PING_1`]

suggesting that in networks with *drive heterogeneity* (different neurons receive different drives), PING oscillations must be created rapidly, within a small number of gamma cycles, if they are to be created at all.

Properties of activity in E-I-networks have been studied extensively; for example, see [11, 12, 60, 153, 154, 166, 181]. In the following sections, we will consider only a few of many interesting aspects of PING rhythms.

30.3   Sparse and random connectivity

Neither of the two cell populations (E and I) synchronizes tightly in Fig. 30.4; this is an effect of heterogeneity in the external drives, and of randomness in the synaptic connectivity. To illustrate this point, Fig. 30.5 shows the same simulation as that of Fig. 30.4, but with all heterogeneity removed. Synchronization now becomes perfect in the limit as $t \to \infty$. This is, of course, not a biologically realistic picture.

Let us ask just how small p_{EI}, p_{IE}, and p_{II} can be before the oscillation is lost. (Note that p_{EE} plays no role yet because we are setting $\hat{g}_{EE} = 0$ for now.) For instance, if we set $p_{EI} = p_{IE} = p_{II} = 0.05$ in the simulation of Fig. 30.4, we obtain Fig. 30.6 — there is only a very faint indication of an oscillation left. However, if we keep the values of p_{EI}, p_{IE}, and p_{II} as in Fig. 30.6, but multiply N_E and N_I by 4 (recall that the strengths of individual synapses are then reduced by 4, see eq. (30.3)), rhythmicity returns; see Fig. 30.7.

For the ability of the network to synchronize and form a rhythm, p_{EE}, p_{EI}, p_{IE}, and p_{II} are not as important as $p_{EE}N_E$, $p_{EI}N_E$, $p_{IE}N_I$, and $p_{II}N_I$, the
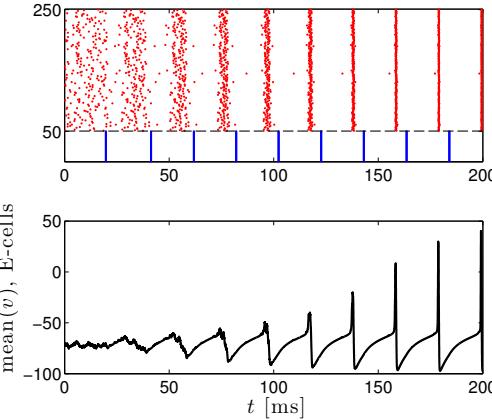
Figure 30.5. *As Fig. 30.4, but with all network heterogeneity removed:*
$\sigma_E = 0$, $p_{EI} = p_{IE} = p_{II} = 1$. [`PING_2`]
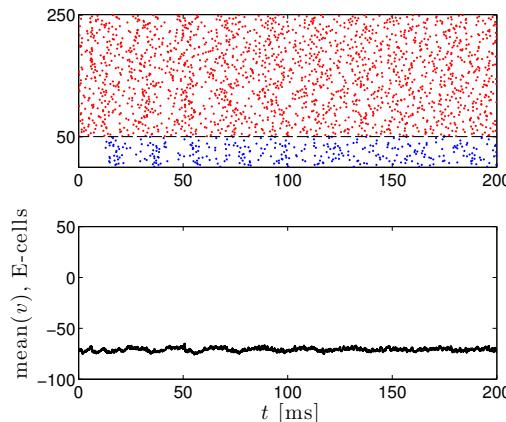
Figure 30.6. *As Fig. 30.4, but with much greater sparseness of the connectivity:* $p_{EI} = p_{IE} = p_{II} = 0.05$. [`PING_3`]

expected numbers of (excitatory or inhibitory) inputs per cell. In fact, $p_{EE}N_E$, $p_{EI}N_E$, $p_{IE}N_I$, and $p_{II}N_I$ largely determine the size of random fluctuations in the input strengths per cell. To show this, consider for instance the sum of all maximal conductances of inhibitory synapses into the i-th E-cell. We denote this sum by $\overline{g}_{Ii}$:

$$\overline{g}_{Ii} = \overline{g}_{IE} \sum_{j=1}^{N_I} Z_{IE,ji}. \tag{30.6}$$
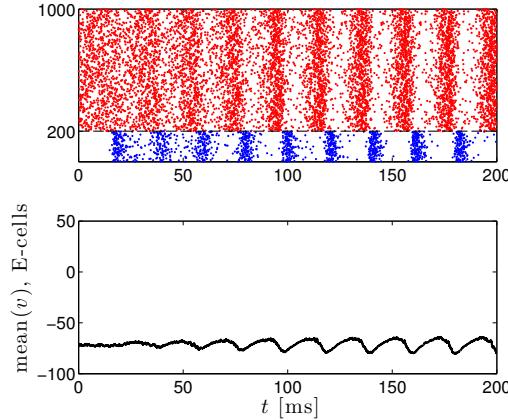
Figure 30.7. *As Fig. 30.6, but for a four times larger network.* [`PING_4`]

Taking expectations on both sides, we obtain

$$E\left(\overline{g}_{Ii}\right) = \overline{g}_{IE}\sum_{j=1}^{N_I} E\left(Z_{IE,ji}\right) = \overline{g}_{IE}p_{IE}N_I. \tag{30.7}$$

Since the $Z_{IE,ji}$ are independent of each other, their variances sum (see Appendix C):

$$\mathrm{var}\left(\overline{g}_{Ii}\right) = \left(\overline{g}_{IE}\right)^2\sum_{j=1}^{N_i}\mathrm{var}(Z_{IE,ji}) = \left(\overline{g}_{IE}\right)^2\sum_{j=1}^{N_I}\left(E\left(Z_{IE,ji}^2\right) - (E(Z_{IE,ji}))^2\right).$$

Since the only possible values of $Z_{IE,ji}$ are 0 and 1, $Z_{IE,ji}^2 = Z_{IE,ji}$, and therefore

$$\left(\overline{g}_{IE}\right)^2\sum_{j=1}^{N_I}\left(E\left(Z_{IE,ji}^2\right) - (E(Z_{IE,ji}))^2\right) =$$

$$\left(\overline{g}_{IE}\right)^2\sum_{j=1}^{N_I}\left(E\left(Z_{IE,ji}\right) - (E(Z_{IE,ji}))^2\right) = \left(\overline{g}_{IE}\right)^2 N_I\left(p_{IE} - p_{IE}^2\right).$$

Taking square roots, we obtain the standard deviation:

$$\mathrm{std}\left(\overline{g}_{Ii}\right) = \overline{g}_{IE}\sqrt{N_I p_{IE}\left(1 - p_{IE}\right)}. \tag{30.8}$$

From (30.7) and (30.8), we obtain the *coefficient of variation* of $\overline{g}_{Ii}$:

$$\mathrm{cv}\left(\overline{g}_{Ii}\right) = \frac{\mathrm{std}\left(\overline{g}_{Ii}\right)}{E(\overline{g}_{Ii})} = \sqrt{\frac{1 - p_{IE}}{p_{IE}N_I}}.$$

For $p_{IE} \ll 1$, therefore,

$$\mathrm{cv}\,(\overline{g}_{Ii}) \approx \sqrt{\frac{1}{p_{IE}N_I}}.$$

Analogous calculations are possible, of course, for the E-to-I, E-to-E, and I-to-I synaptic connections. This completes our argument showing that $p_{EE}N_E$, $p_{EI}N_E$, $p_{IE}N_I$, and $p_{II}N_I$ determine, in a sparse network, the size of variations in synaptic input strengths per cell.

One might summarize the conclusion by saying that it is not the *sparseness* of connectivity that hinders synchronization, but its *randomness*. In fact, what really matters is one particular aspect of that randomness, namely the variability in the numbers of excitatory and inhibitory inputs per cell. This point is illustrated by Fig. 30.8. The middle panel of the figure shows results of a simulation in which connectivity is so sparse that the *mean* number of excitatory and inhibitory inputs per cell is 1. Not surprisingly, synchronization is lost. The bottom panel of the figure shows results of a simulation of a very similar network, in which however the *exact* number of excitatory and inhibitory inputs per cell equals 1. The E- and I-cells from which these inputs originate are still chosen at random, but the fluctuations in the numbers of inputs per cell have been eliminated. Pronounced rhythmicity is recovered. The point is made again, more strikingly, by Fig. 30.9, which shows results of the same simulations, but continued over a long time interval. (Only the last 200 ms of simulated time are shown.) Synchronization eventually becomes perfect with just one single excitatory and inhibitory input per cell!

30.4   Strengths of external drives and the suppression boundary

For the PING mechanism to work, the I-cells should not fire without being prompted by an E-cell spike volley. In the notation used earlier, this roughly means that $\overline{I}_E$ must be large enough, or $\overline{I}_I$ small enough. If $\overline{I}_E$ is fixed, rhythmicity is lost as $\overline{I}_I$ rises. Similarly, if $\overline{I}_I$ is fixed, rhythmicity is lost as $\overline{I}_E$ falls. In idealized circumstances, there is a sharply defined boundary in parameter space, with the property that PING is possible on one side of the boundary, but not on the other [12]. We called this the *suppression boundary* in [12], and hypothesized in [10] that it might play a role in brain function because it allows toggling between non-rhythmic and rhythmic states with only small changes in parameters. In less idealized circumstances, with heterogeneity in external drives and randomness in synaptic connectivity, the "suppression boundary" is not sharply defined. There is a more gradual, but often still fairly abrupt transition from rhythmic to non-rhythmic states as the I-cells become more excited, or as the E-cells become less excited. Figures 30.10 and 30.11 illustrate the fairly abrupt loss of rhythmicity as $\overline{I}_I$ is raised. Note that Fig. 30.10 looks quite similar to Fig. 30.4 — the fact that the I-cells have more drive than in Fig. 30.4 is of little consequence. However, as $\overline{I}_I$ rises from 0.7 (Fig. 30.10) to 0.9 (Fig. 30.11), rhythmicity is largely lost.
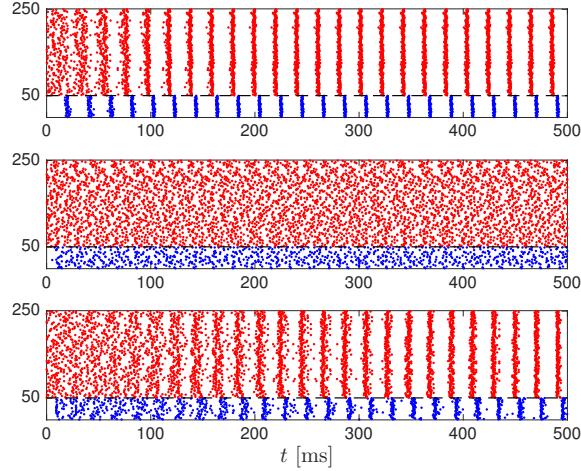
Figure 30.8. *Top panel: As in Fig. 30.4 (a longer time interval is simulated here), but with heterogeneity in the drive to the E-cells removed, i.e., $\sigma_E = 0$. The failure to reach perfect synchrony is now exclusively due to the randomness of the synaptic connections. Middle panel: A similar simulation, but with $p_{EI} = 1/200$, $p_{IE} = 1/50$, and $p_{II} = 1/50$, so the* expected *numbers of excitatory and inhibitory inputs per cell are 1. Bottom panel: Same as middle panel, but now the* actual *numbers of excitatory and inhibitory inputs per cell are 1. Note that there is very little, if any, rhythmicity in the middle panel, while pronounced rhythmicity emerges in the bottom panel.* [PING_5]
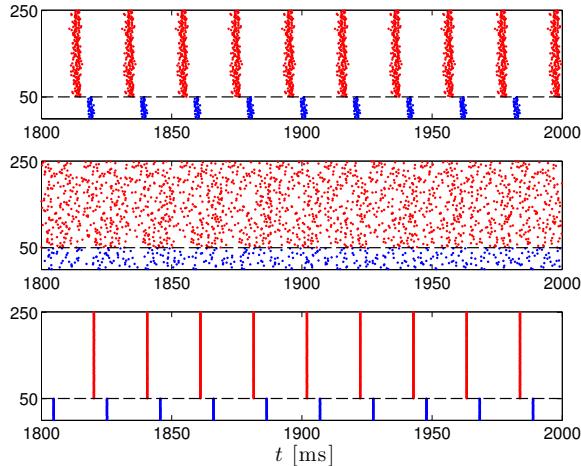
Figure 30.9. *Same as Fig. 30.8, but with simulations continued up to time 2000. Only the last 200 ms of simulated time are shown.* [PING_6]
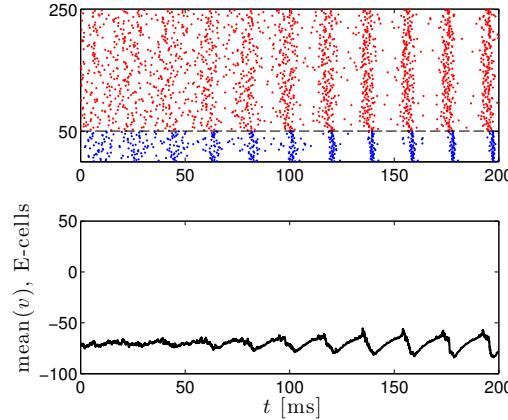
Figure 30.10. *Same as Fig. 30.4, but with $\overline{I}_I = 0.7$, $\sigma_I = 0.05$.* [PING_7]
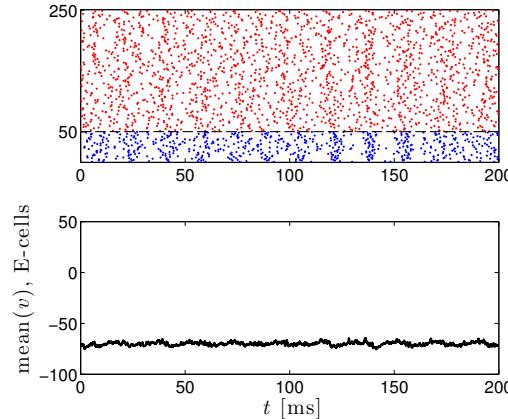
Figure 30.11. *Same as Fig. 30.4, but with $\overline{I}_I = 0.9$, $\sigma_I = 0.05$.* [PING_8]

30.5   Recurrent inhibition

By *recurrent inhibition*, we mean I-to-I synapses here. When $\hat{g}_{II}$ is set to zero in the simulation of Fig. 30.4, i.e., when recurrent inhibition is eliminated, the result is largely unchanged; the frequency rises slightly (exercise 4). On the other hand, by tripling $\hat{g}_{II}$ one can restore rhythmicity in Fig. 30.11 (exercise 5). Thus I-to-I connectivity can play the role of "calming" the I-cells and thereby allowing the PING mechanism to work when the external drive to the I-cells would otherwise be too strong, but it is not needed for the emergence of a PING rhythm when the drive to the I-cells is weak enough.
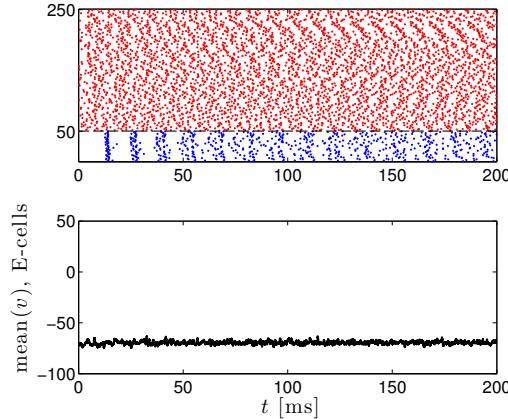
Figure 30.12. *Same as Fig. 30.4, but with $\hat{g}_{EE} = 0.25$, $p_{EE} = 0.5$.* `[PING_9]`

30.6   Recurrent excitation

Up to this point, we have set $\hat{g}_{EE} = 0$ in this chapter, so there have not been any E-to-E synaptic connections. When we add weak E-to-E connections, with the same time constants as for the E-to-I connections ($\tau_{r,E} = \tau_{\text{peak},E} = 0.5$ ms, $\tau_{d,E} = 3$ ms), the PING rhythm is barely affected. Stronger E-to-E connections destroy the rhythm; see Fig. 30.12. This is in contrast with the Wilson-Cowan model of Chapter 22, which *requires* recurrent excitation for oscillations.

Exercises

30.1. Vary the baseline parameters perturbed in Table 30.1, and see how the results change.

30.2. Explain why the expectation of (30.4) is $p_{EI}N_E$.

30.3. Explain why $\hat{g}_{EI}$ is the expected value of the sum of all maximal conductances associated with excitatory synaptic inputs into a given I-cell.

30.4. ($*$) Verify that the rhythm in Fig. 30.4 is largely unchanged when $\hat{g}_{II}$ is set to zero.

30.5. ($*$) Verify that the rhythm in Fig. 30.11 is restored when $\hat{g}_{II}$ is tripled.

30.6. Explain why one would *expect* that short recurrent excitatory synapses would not affect PING rhythms much.

30.7. ($*$) ($\dagger$) PING rhythms in our model networks have very regular population frequencies; that is, the times between population spike volleys are nearly constant. Experimentally recorded gamma rhythms are much less regular; see for instance the top trace of Fig. 30.2.

One can try to introduce more variability by adding to the drives $I_{E,i}$ a sin-

gle discrete Ornstein-Uhlenbeck process $S(t)$ (independent of i), as defined by eqs. (C.20)–(C.22) in Appendix C.6. This would model global fluctuations in the excitability of E-cells. In a living brain, such fluctuations could result from *neuromodulation*. (In general, the word *neuromodulation* denotes the regulation of a whole population of neurons by a diffusely released neurotransmitter.)

Explore computationally whether you can set the parameters of the discrete Ornstein-Uhlenbeck process so that the PING rhythm is not destroyed, but its frequency becomes significantly more variable.

30.8. (∗) What happens if you make the inhibitory synapses in the simulation of Fig. 30.4 much stronger, but also much faster, say $\tau_{r,I} = \tau_{\mathrm{peak},I} = 0.5\,\mathrm{ms}$, $\tau_{d,I} = 3\,\mathrm{ms}$? Can you still get a gamma rhythm?